Calibration of a semi-distributed model for conjunctive simulation of surface and groundwater flows

Calibration d`un modèle semi-distribué pour la simulation conjointe de flux superficielles et souterraines

EVANGELOS ROZOS, ANDREAS EFSTRATIADIS*, IOANNIS NALBANTIS & DEMETRIS KOUTSOYIANNIS

Department of Water Resources, School of Civil Engineering

National Technical University of Athens

Heroon Polytechneiou 5, GR-15780 Zographou, Greece

tel: +30 210 772 2861, fax: +30 210 772 2832

(* Corresponding author, andreas@itia.ntua.gr)

Paper submitted to Hydrological Sciences Journal (HSJ2114)

June 2004

Abstract

A hydrological simulation model was developed for conjunctive representation of surface and groundwater processes. It comprises a conceptual soil moisture accounting module, based on an enhanced version of the Thornthwaite model for the soil moisture reservoir, a Darcian multi-cell groundwater flow module and a module for partitioning water abstractions among water resources. The resulting integrated scheme is highly flexible in the choice of time (i.e. monthly to daily) and space scales (catchment scale, aquifer scale). Model calibration involved successive phases of manual and automatic sessions. For the latter, an innovative optimization method called evolutionary annealing-simplex algorithm is devised. The objective function involves weighted goodness-of-fit criteria for multiple variables with different observation periods, as well as penalty terms for restricting unrealistic water storage trends and deviations from observed intermittency of spring flows. Checks of the unmeasured catchment responses through manually changing parameter bounds guided choosing final parameter sets. The model is applied to the particularly complex Boeoticos Kephisos basin, Greece, where it accurately reproduced the main basin response, i.e. the runoff at its outlet, and also other important components. Emphasis on the principle of parsimony is put which resulted in a computationally effective modeling. This is crucial since the model is to be integrated within a stochastic simulation framework.

Key words: conjunctive surface and groundwater use; Thornthwaite model; multi-cell model; global optimization; evolutionary annealing-simplex algorithm; hydrological simulation.

Résumé

Un modèle de simulation hydrologique a été développé pour la représentation conjointe de processus superficiels et souterrains. Ceci comprend un module conceptuel pour le bilan hydrique du sol, basé sur une version renforcée du réservoir Thornthwaite, un module multi-cellule de flux souterrain Darcien et un module qui distribue les prélèvements d`eau parmi ses différentes ressources. Le schéma integré qui en résulte est très flexible pour ce qui est du choix de l`échelle de temps (mois, jour) et d' espace (bassin versant, aquifère). La calibration du modèle comprend des phases alternantes de sessions manuelles et automatiques. En ce qui concerne les dernières, une méthode originale

d`optimisation est inventée qui s`appèle algorithme évolutionnaire de recuit simulé-simplèxe. Ceci emploie une fonction objectif originale qui comprend des critères d' ajustément pondérés pour des variables multiples et des périodes d`observation variables. La fonction comprend aussi des termes de peine qui imposent des restrictions aux tendances irréalistes du stock d`eau et aux déviations de l`intermittence entre observée et modélisée du débit de sources. Le choix des valeurs finales des paramètres est guidé par des contrôles des sorties non mesurées en faisant varier manuellement les limites des paramètres. Le modèle est appliqué à un bassin versant grec complexe, ceci de Boeoticos Képhisos. Il a reproduit avec précision la réponse principale du bassin, qui est le débit à son exutoire, mais aussi d`autres composantes importantes. On focalise sur le principe de parcimonie ce qui conduit à une modélisation très efficace. Cela est crucial puisque le modèle est destiné à être integré dans un système de simulation stochastique.

Mots-clefs: usage conjointe de flux superficielles et souterraines; modèle Thornthwaite; modèle multi-cellule; optimisation globale; algorithme évolutionnaire de recuit simulé-simplèxe; simulation hydrologique.

INTRODUCTION

Integrated management of water resource systems requires a conjunctive representation of surface and groundwater dynamics, especially when combined uses are involved. This stands as one of the most challenging issues in hydrological modeling. Traditionally, to simulate water fluxes, a hydrosystem is represented by storage and conveyance components for which inflow time series, whether they originate from surface or groundwater resources, are pre-computed and entered externally. However, this may be insufficient due to decision-related interactions between surface and groundwater flows. A typical example is when inflows to a reservoir are significantly reduced due to upstream groundwater abstractions. In that case, conjunctive simulation of both surface and groundwater processes is needed, to assess the impacts of the abstractions to the reservoir yield.

A mathematical framework for conjunctive modeling of surface and groundwater flows is presented. This hydrological simulator consists of three components: (a) a semi-distributed soil moisture accounting module for surface processes, (b) a multi-cell groundwater module, and (c) a

demand-partitioning module. The synthetic model is established for the Boeoticos Kephisos river basin, the most important characteristic of which is the existence of an extended karstic aquifer that contributes significantly to the total basin streamflow. Both surface and groundwater resources supply irrigation water locally as well as drinking water to Athens. Furthermore, the basin's surface outflows account for most of the inflow of Lake Yliki, which is the second largest reservoir of the Athens water supply system. Hence, the interactions between surface and groundwater flows and abstractions, in addition to the need for a rational water management, impose the adoption of a conjunctive simulation scheme. The hydrological simulator is designed as part of an integrated decision support tool (DSS) for the management of the water resource system of Athens (Koutsoyiannis *et al.*, 2002). The DSS yields the optimal operation of the hydrosystem, employing stochastic simulation within an optimization scheme. Inflow series, including those of Lake Yliki, are synthetically generated through a stochastic module of the DSS. Until now, several attempts were made to integrate a hydrological model within the DSS, in order to estimate the impacts of water supply and irrigation abstractions to Yliki inflows (Nalbantis *et al.*, 2002). Among these were a lumped simulation scheme and a distributed model, implemented within the MODFLOW package (Nalbantis & Rozos, 2000). While the lumped model performed relatively well regarding its prediction accuracy, it was not able to represent the basin processes at the desired spatial scale, and especially the spring flow dynamics that are directly affected by the water supply abstractions. On the other hand, the MODFLOW model, although useful for better spatial information treatment, was ineffective regarding its ability to run in stochastic simulation mode. Hence, the requirement was to build a model that provides a satisfactory prediction of the hydrological processes, while remaining at the same time computationally effective.

In addition to the model formulation, the paper is focused on the parameter estimation procedure. A hybrid approach that combines manual and automatic calibration is presented, aiming at restricting the uncertainties due to the complexity of the physical system and the lack of reliable and systematic spatially distributed data. The objective function attempts to incorporate all information concerning the watershed response, by means of measured hydrographs and, to a lesser extent, groundwater level observations. Finally, for the automatic calibration procedure, a new heuristic

evolutionary optimization algorithm is introduced, where a generalized downhill simplex scheme is effectively coupled with a simulated annealing strategy.

The paper is organized in five sections. Section 2 describes the mathematical structure, the assumptions and the integration of the three components of the model. Section 3 deals with the optimization algorithm. In Section 4 we present the application of the model to the Boeoticos Kephisos river basin and discuss the calibration procedure and the results. Finally, Section 5 summarizes the conclusions and provides some proposals for further research.

MATHEMATICAL FRAMEWORK

Hydrological simulation through conceptual water balance models

Simulation models help understand mechanisms regarding water fluxes; moreover, they serve to predict the behavior of the physical system, under a given set of naturally occurring circumstances (Beven, 1989). Typically, such models are applied at the watershed or the aquifer scale; but conjunctive simulations are relatively rare. This is due to the different physical characteristics of the surface and groundwater processes. For example, in the usual case of porous aquifers, groundwater velocities are some orders of magnitude smaller than the surface ones thus imposing proper adaptation of temporal and spatial scales. Another typical example is when spring runoff to streamflow is negligible, as compared to flood runoff.

In typical practical applications, conceptual models, with an a priori specified mathematical structure based on empirical hypotheses, are preferable to physics-based ones, which are restrained by the large amount of spatially distributed data required to represent the heterogeneity of physical processes. It is widely recognized that the reliability of conceptual models is strongly dependent on the adequacy of the calibration procedure employed (e.g., Sorooshian and Gupta, 1983; Yapo *et al.*, 1998). Hence, the confidence to these models depends on the predictive uncertainty remaining after the calibration. Other sources of uncertainty are the structural complexity of the model and the level of information contained within the observations used as inputs. Therefore, when formulating and calibrating a hydrological model, the key point is to find a good equilibrium between model complexity and predictive uncertainty, given the available data (Wagener *et al.*, 2001). A successful

calibration should involve sufficient predictive capacity of the model, in addition to a realistic parameter set. The former ensures the reproduction of catchment behavior with satisfactory accuracy, while the latter ensures that the model parameters, albeit conceptual, are representative of the average characteristics of the basin.

Surface water simulation model

Water balance models for surface hydrology processes have been developed at various scales and to varying degrees of complexity (Xu & Singh, 1998), ranging from relatively complex models with 10 to 15 parameters for arid regions to very simple ones, for humid regions in temperate zones (Makhlouf and Michel, 1994). Most of them represent the transformation of rainfall to runoff through one or more conceptual reservoirs, based on the pioneer work of Thornthwaite (1948) and Thornthwaite & Mather (1955). Specifically, the Thornthwaite model was initially developed to estimate monthly actual evapotranspiration E_t, using monthly values of precipitation, P_t, and potential evapotranspiration, E_{Pt} (a schematic illustration of the model is given in Figure 1, left). The whole basin is represented by a conceptual soil moisture reservoir of capacity K, which is the only parameter of the model. When the soil is saturated, i.e. the storage exceeds the capacity K, the reservoir spills; this spill corresponds to the basin runoff, Q_t. The evapotranspiration demand is first satisfied through precipitation and, at a second stage, if necessary, through the available soil moisture. In that case, it is assumed that the soil evaporation rate, symbolized E_{St}, is proportional to the deficit $E_{Pt} - P_t$ and the storage ratio S_t / K.

The above approach is suitable only for catchments without significant groundwater contribution, since it cannot represent the deep percolation process, neither permanent flows. Moreover, when applying this model in arid or semi-arid regions, the assumption that the entire precipitation is transformed into evapotranspiration becomes unrealistic. This is because the monthly precipitation occurs through few storm events at much finer time scales (e.g. hourly, daily); in such scales, precipitation usually exceeds potential evapotranspiration, whereas on a monthly basis this may be not true.

To cope with the above drawbacks, several modifications were implemented to the original model, as shown in Figure 1, right. In the modified scheme, the total runoff, Q_t, is divided into two parts: a direct component, D_t, occurring during storm events, and the quick subsurface flow (interflow), I_t. The former occurs when the actual soil moisture storage exceeds the reservoir capacity, now symbolized as K_2 instead of K. The latter is represented by a horizontal orifice, lying at level $K_1 < K_2$, and its rate is assumed proportional to $S_t - K_1$ and a recession coefficient λ, i.e. $I_t = \lambda (S_t - K_1)$. Additionally, the modified soil moisture reservoir contains a bottom orifice, for percolation, G_t, to deeper zones. Similarly to the interflow, percolation rate is assumed proportional to the actual moisture storage S_t and a recession coefficient μ, i.e. $G_t = \mu S_t$. Finally, the modified model imposes a maximum fraction, ε, of precipitation that can be directly evaporated. Therefore, the soil evaporation rate is estimated by:

$$E_{St} = \frac{\max (0, E_{Pt} - \varepsilon P_t)}{K_2} S_t \tag{1}$$

For $\varepsilon = 1$, the above relationship is identical to that of the Thornthwaite model. At the beginning of each time step, the precipitation excess $\Delta P_t = P_t - \min (\varepsilon P_t, E_{Pt})$ is added to the actual soil moisture storage. To cope with typical time scale drawbacks, the calculation of water balance components is implemented analytically, by formulating a first order differential equation, based on the mass continuity principle. This equation is written as:

$$\frac{1}{\Delta} \frac{\mathrm{d}S}{\mathrm{d}\tau} = \lambda K_1 - \left(\lambda + \mu + \frac{\max (0, E_{Pt} - \varepsilon P_t)}{K_2} \right) S \tag{2}$$

where Δ is the time resolution (e.g. one month) and τ is dimensionless time, in the interval [0, 1]. By solving (2), assuming as initial storage the amount $S_{t-1} + \Delta P_t$, we obtain the soil moisture storage at the end of the actual time step. An important assumption is that within the time interval the soil moisture is allowed to exceed the reservoir capacity. Practically, this excess represents water that cannot be absorbed by the saturated soil and is first let to pond and then evaporate or infiltrate. This assumption enables the generation of more realistic output series, the variability of which is consistent with the variability of precipitation. After the calculation of hydrological outflows given by (2), the soil moisture excess (if this still exists) is spilled and contributes to the streamflow as direct runoff.

In conclusion, the modified model, besides the direct runoff and the actual evapotranspiration, estimates also the interflow and the percolation, by using five parameters in total, namely the interflow threshold K_1, the soil storage capacity K_2, the recession rates λ and μ, and the fraction, ε (if the model is applied in a finer than monthly scale, one can set $\varepsilon = 1$).

Groundwater simulation model

The groundwater flow simulation is based on the concept of multi-cell models that stand between conceptual and physical-based models (Bear, 1979, pp. 447-454). They resemble the finite difference models with small number of cells, but they have some fundamental differences. The geometry and discretization of multi-cell models is very flexible and, although the cells are usually rectangular, they may correspond to aquifer regions with any shape. The discretization is mainly imposed by the available hydrological information and the water management plans. Moreover, model parameters are rather conceptual, thus needing calibration. The dynamics of multi-cell models arise from the application of water balance equations in all cells, in combination with Darcy's law; on the other hand, although water levels do not correspond to physical magnitudes, their variability may only be used to estimate real groundwater level trends.

In the proposed approach, which is suitable for phreatic conditions, a network is formulated consisting of storage elements (tanks) and conveyance elements (conduits). The properties of each tank i are its centroid coordinates, its base area, F_i, that equals the area of the corresponding aquifer multiplied by its specific yield, S_Y. The properties of each conduit that links tank i with tank j are its conductivity, C_{ij} (expressed in velocity units), its length, L_{ij}, and its cross-sectional area, A_{ij}, which is identical to the corresponding aquifer cross-section area. Note that both A_{ij} and L_{ij} correspond to real geometrical magnitudes, which are calculated according to the centroid coordinates of model tanks and the aquifer thickness.

The neighboring tanks 1 and 2 in Figure 2 correspond to the aquifer regions 1 and 2. Their base areas are F_1, F_2 and the water levels in them are w_1 and w_2, respectively. The discharge, Q_{12}, occurring from tank 1 to tank 2, is estimated via the Darcy's equation, i.e. $Q_{12} = C_{12} A_{12} (w_1 - w_2) / L_{12}$, where C_{12} is the conductivity of conduit 1-2, L_{12} is the conduit length, and A_{12} is the cross-section area between

aquifer regions 1 and 2. After time δt, the water level changes (fall or rise) in tanks 1 and 2 are $\Delta w_1 \approx - Q_{12}\, \delta t / F_1$ and $\Delta w_2 \approx Q_{12}\, \delta t / F_2$, respectively.

The groundwater flow problem is solved via an explicit numerical scheme, by adopting a small time step δt within which the influence of the variation of water levels to the groundwater discharge can be neglected. To achieve the optimum speed and stability of the arithmetic solution, the time step is tuned throughout the simulation by using a maximum allowed water level change, Δw_{max}, within a time interval, a tolerance, a, and a multiplier, β. If $\Delta w_{max}\,(1 - a) < \Delta w_i < \Delta w_{max}\,(1 + a)$ for each tank i, the time step remains unchanged, otherwise the time step is either multiplied or divided by β. The initial time step, δt_0, the maximum allowed water level change, Δw_{max}, the tolerance, a, and the time step multiplier, β, are user-specified.

The initial conditions refer to initial water level values in tanks, whereas the boundary conditions refer to tanks with constant level. The latter can be modeled through a tank of very large base. Hence, a spring is modeled as a tank of very large base and the simulated series of the slight changes of level can be directly transformed to spring hydrographs. The stress at each tank may be positive (recharge) or negative (pumping).

Model integration within a conjunctive surface-groundwater simulation scheme

The models developed were integrated within a conjunctive simulation scheme, based on a semi-distributed concept, as illustrated in Figure 3. The model was applied on a monthly scale; however, we believe that a daily scale would also be suitable. On the other hand, a finer time step is not recommended, because it would need routing procedures that are not incorporated in this scheme. The whole catchment is divided into spatial subunits with similar hydrological and morphological characteristics. These so-called hydrological response units (HRUs) do not necessary correspond to physical sub-basins; they are rather conceptual elements, the dynamics of which are modeled via a soil moisture accounting reservoir. On the other hand, the aquifer is divided in cells, each one represented by a conceptual groundwater tank.

Each cell is supplied by the percolation of a specific HRU; but the same HRU can supply more than one cells. Supposing that percolation is expressed in terms of equivalent water depth, its

distribution is made proportionally to the area of each cell. This feature increases the flexibility of the model since it allows using different spatial analysis for the surface and groundwater processes. Thus, a detailed scheme for the representation of groundwater fluxes can be easily coupled with a coarse one for the simulation of the surface ones; even a lumped approach (i.e. a single HRU) may be adequate, provided that the catchment characteristics are homogenous. To achieve numerical stability in groundwater simulation, a small computational step δt has to be adopted, which is much finer than the initial simulation step, Δt (monthly or daily). Hence, the stress inputs (percolation and pumping) that are given at a resolution Δt are uniformly disaggregated, in order to be consistent with δt. On the other hand, the output series of the multi-cell model are aggregated at the specified simulation step, Δt.

The total streamflow is estimated by adding the spring outflows to the direct runoff and the interflow components, while the water abstractions are made either from surface or groundwater resources. The implementation of the former is trivial whereas the latter require some modeling when combined abstractions exist. Let R_t be the water demand at time interval t, which is primarily fulfilled via surface abstractions and secondly via pumping, and let Q_t be the actual streamflow, part of which arises from spring outflows. If $Q_t < R_t$, the actual deficit, $R_t - Q_t$, has to be fulfilled via pumping. However, pumping reduces water level at the groundwater tanks; this reduces the spring outflow and, consequently, the total runoff. This imposes further pumping, and so on. For this reason, the simulation scheme is coupled with a demand-partitioning model, which is executed in several cycles, until the streamflow value stabilizes. Usually, only one or two cycles are needed for convergence.

THE OPTIMIZATION ALGORITHM

General principles

The recent development of effective and robust global optimization techniques enables the automatic calibration of hydrological models. Franchini *et al.* (1998) make a thorough review of these techniques, which aim to handle the usual handicaps of nonlinear optimization, such as the existence of multiple local optima at various scales and parameter interactions.

The calibration of the conjunctive simulation model was implemented through the evolutionary annealing-simplex algorithm, which is a probabilistic heuristic global optimization technique that

incorporates strategies from different methodological approaches, enhancing them with some original elements (Efstratiadis, 2001; Efstratiadis & Koutsoyiannis, 2002). This algorithm was successfully applied to a variety of benchmark functions as well as some simple hydrological applications, and proved very reliable in locating the global optimum, requiring reasonable computational effort. But till now, it was not tested in such a challenging real-world model calibration problem (some information about the peculiarities of this problem are given in section "Model calibration"). Its main principle is to effectively couple the robustness of simulated annealing in problems with rough search space, with the efficiency of local search methods in simple ones. There are only few references in literature on how to implement such combined schemes; among them, we distinguish the simplex-annealing algorithms of Press *et al.* (1992, pp. 451-455), Kvaniscka & Pospichal (1997) and Pan & Wu (1998). Simulated annealing is a stochastic optimization technique based on an analogy with the homonymous thermodynamical process. During the cooling process of a metal, nature's strategy is to both decrease and increase its energy, enabling thus to escape from a local minimum energy state in favor of finding a better one. This principle is implemented according to a probabilistic law, depending on the temperature; the lower is the temperature, the less likely is a significant "uphill" transition. To apply a similar strategy within an optimization procedure, it is required to use a control parameter, analogous of the temperature, and an annealing cooling schedule that describes the gradual temperature reduction. It can be proven that, assuming a large initial temperature and a proper schedule, a simulated annealing procedure asymptotically converges to the global optimum. Hence, an annealing-based algorithm can escape from local optima and pass through various regions of attraction until locating the global optimum; but in so doing it sacrifices efficiency.

On the other hand, deterministic search methods, either gradient-based or direct (i.e., derivative-free), can easily converge to a local stationary point, but they have no way of getting out of it. A well-known direct search method is the downhill simplex algorithm of Nelder & Mead (1965). Its core is an evolving pattern of $n + 1$ points (assumed as the vertices of a simplex) that span the n-dimensional search space. The simplex explores the feasible space either by reflecting, contracting or expanding away from the actually worst vertex, or by shrinking towards the best one. An appropriate sequence of such movements guides the simplex to the nearest local minimum, provided that the search space is

relatively smooth. Due to its efficiency, the principles of the Nelder-Mead method have been incorporated into some global optimization schemes, such as the widely used shuffled complex evolution algorithm of Duan *et al.* (1992).

Description of the algorithm

The proposed algorithm is based on the following three concepts: (a) an evolutionary search strategy, (b) a set of combined (both deterministic and stochastic) transition rules, either downhill or uphill, mainly implemented within a simplex-based evolving pattern, and (c) an adaptive annealing cooling schedule that regulates the "temperature" of the system, determining the degree of randomness through the evolution procedure.

To initialize, a population of $m \geq n + 1$ points is randomly generated into the feasible space, where n is the problem dimension. This population is gradually evolved by, usually, replacing just one existing point by a new one (adopting the terminology of genetic algorithms, the former will referred as "parent", whereas the latter as "offspring"). Note that according to the simulated annealing principle, an "offspring" should not necessarily be better than its "parent". Considering a minimization problem, a typical iteration cycle consists of the following steps:

Step 1: The minimum, $f_{\min}$, and maximum, $f_{\max}$, values of the objective function, f, within the actual population are drawn and the system temperature, T, is re-evaluated so that it never exceeds the amount $\xi\,(f_{\max} - f_{\min})$, where $\xi \geq 1$ is a parameter of the annealing schedule. This restriction prevents the "temperature" taking extremely high values, which would drastically reduce the speed of the algorithm due to the fact that the searching procedure would become extremely random.

Step 2: A set of $n + 1$ points is randomly selected from the actual population. This set will next referred as a simplex and symbolized as $S = \{\mathbf{x}_1, \mathbf{x}_2, \ldots, \mathbf{x}_{n+1}\}$, where $f(\mathbf{x}_1)$ corresponds to the best (lowest) and $f(\mathbf{x}_{n+1})$ to the worst function value.

Step 3: From the subset $S - \{\mathbf{x}_1\}$, we choose as candidate parent the point $\mathbf{x}_w$ that maximizes the probabilistic criterion:

$$g(\mathbf{x}) = f(\mathbf{x}) + u\,T \tag{3}$$

where u is a random number uniformly distributed in the interval [0, 1]. By adding a random component to the objective function f, relative to the actual temperature T, the algorithm behaves as in between random and downhill search. In reality, the evaluation criteria are now based on a transformed objective space, which may be much smoother than the original one, thus providing more flexibility to the search procedure, especially at the early stages of it (i.e., when temperature is high).

Step 4: A new point, $\mathbf{x}_r$ is generated by reflecting the simplex away from $\mathbf{x}_w$, according to the formula:

$$\mathbf{x}_r = \mathbf{g} + (0.5 + u)\,(\mathbf{g} - \mathbf{x}_w) \tag{4}$$

where $\mathbf{g}$ is the centroid of the subset $S - \{\mathbf{x}_w\}$.

Step 5: If $f(\mathbf{x}_r) < f(\mathbf{x}_w)$, $\mathbf{x}_r$ replaces $\mathbf{x}_w$ in the actual population. Next, two cases arise. If $f(\mathbf{x}_r) < f(\mathbf{x}_1)$, i.e. the reflection point is better than the current best vertex, the difference $\mathbf{x}_r - \mathbf{g}$ denotes a direction of function minimization or, equivalently, an estimation of the gradient. This fact is of high importance, because it enables the search procedure to progress quickly towards a local minimum. Generally, the location of the gradient in a rough search space may be extremely difficult, especially when the problem is of high dimension. Therefore, whenever the gradient is found, a sequence of "expansion" steps are implemented towards the direction of function minimization, according to the simple formula:

$$\mathbf{x}_e = \mathbf{g} + \varphi[s]\,(\mathbf{x}_r - \mathbf{g}) \tag{5}$$

where $\varphi[s] = \varphi[s - 1] + u$, with $\varphi[0] = 1$. The expansion continues as long as the function value improves, thus accelerating significantly the search procedure. The second case arises when $f(\mathbf{x}_r) > f(\mathbf{x}_1)$, indicating that a local minimum is in the neighborhood of $\mathbf{x}_1$. Then, an offspring is generated as follows:

$$\mathbf{x}_c = \mathbf{g} + (0.25 + 0.5\,u)\,(\mathbf{x}_r - \mathbf{g}) \tag{6}$$

Adopting the terminology of Nelder & Mead, the above configuration is called outside contraction. If $f(\mathbf{x}_e) < f(\mathbf{x}_r)$ or $f(\mathbf{x}_c) < f(\mathbf{x}_r)$, the new point (either $\mathbf{x}_e$ or $\mathbf{x}_c$) replaces $\mathbf{x}_r$ in the actual population.

Step 6: If $f(\mathbf{x}_r) > f(\mathbf{x}_w)$, we use the probabilistic criterion (3) to accept or reject $\mathbf{x}_r$ as candidate offspring. Hence, if $g(\mathbf{x}_r) > g(\mathbf{x}_w)$, $\mathbf{x}_r$ is rejected and the simplex is inside contracted as:

$$\mathbf{x}'_c = \mathbf{g} - (0.25 + 0.5\,u)\,(\mathbf{g} - \mathbf{x}_r) \tag{7}$$

If $f(\mathbf{x}'_c) > f(\mathbf{x}_{n+1})$, i.e. $\mathbf{x}'_c$ is worse even than the actual worst vertex, the simplex shrinks towards the actual best vertex $\mathbf{x}_1$, such as $\mathbf{x}_{s,i} = 0.5\,(\mathbf{x}_1 + \mathbf{x}_i)$ for $i = 2, \ldots, n+1$. A simplex volume reduction indicates that a local optimum is surrounded. In that case, more than one offsprings are generated, and the system temperature is reduced by ψ, which is a second parameter of the annealing schedule, taking values into the interval 0.90-0.99. A slight reduction rate prevents temperature taking extremely low values. Hence, the searching procedure is prevented from becoming too deterministic, thus avoiding early convergence to a local optimum.

Step 7: If $g(\mathbf{x}_r) < g(\mathbf{x}_w)$, $\mathbf{x}_r$ is accepted even if it deteriorates the function value. Next, a given number of uphill movements are implemented using a formula analogous to (5), until passing the hill and finding a new region of attraction. This strategy, which is quite similar to those introduced by Pan & Wu (1998), makes the simplex easily escaping from the current local minimum and search for neighboring local minima.

Step 8: If it is not possible to locate a better offspring, either at the downhill or uphill direction, a random point is generated within the boundaries of the actual population and replaces $\mathbf{x}_r$ according to a mutation probability p_m.

Only the main issues of the algorithm are given above; for more details, the reader may refer to the original work of Efstratiadis (2001) and Efstratiadis & Koutsoyiannis (2002). The main configurations of the search strategy are illustrated in the graphical example of Figure 4.

APPLICATION OF THE MODEL TO THE BOEOTICOS KEPHISOS RIVER BASIN

Description of the study area

The Boeoticos Kephisos river basin, illustrated in Figure 5, lies on the Eastern Sterea Hellas, north of Athens, and drains an area of 1987 km^2. The catchment geology comprises heavily karstified limestone, practically developed on the mountainous and semi-mountainous areas of the basin, and alluvial deposits, lying in the plain areas. Due to its karstic background, the watershed has a significant groundwater yield. The main discharge points are large karstic springs in the upper and middle part of the basin, the most important of which are shown in Figure 5. These account for more than half of the catchment runoff. Moreover, an unknown part of groundwater is conducted to the sea, from the NE

boundary of the basin. A direct measurement of those outflows is infeasible since their front is too extended.

The river network of the basin originates from altitudes as high as 2400 m and reaches downstream to a plain with an area of about 250 km^2 and a mean ground elevation of 95 m. Prior to 1860, the plain was permanently flooded by the basin's runoff, thus giving rise to the formulation of a shallow lake (Kopais) with a mean area of about 150 km^2. However, during periods of high flows, the lake expanded to 250 km^2 as the capacity of karstic sinkholes was insufficient. Effective drainage works were initiated in ancient times (2000 B.C.), as reported by Strabo, the geographer (Koukis & Koutsoyiannis, 1997). The problem was permanently remedied only by the end of 19th century, after the construction of an extended drainage network and a tunnel (Karditsa tunnel) that conveys the entire surface water resources of the basin to the external Lake Yliki. From 1950 to 1980, this lake was the major water storage project of Athens. Today, Lake Yliki is part of a complex hydrosystem, extending on an area of more than 4000 km^2 and comprising three additional reservoirs, 350 km of aqueducts, 15 pumping stations, four treatment plants and a hundred of boreholes. Besides, some of the most important supply boreholes are located at the Vassilika-Parori region, just upstream of the Mavroneri springs. These boreholes were drilled in the early 1990's, within the frame of emergent measures taken during a severe drought in the period from 1989 to 1994, at the end of which almost all surface resources dried out. Due to a significant reduction of precipitation, in addition to major abstractions through the Vassilika-Parori boreholes, the discharge of Mavroneri springs was totally interrupted during 1990 and 1993, thus resulting to various social and environmental problems.

In addition to drinking water for Athens, the surface and groundwater resources of the study basin are used for irrigation. The total irrigated area is 325 km^2 and the total irrigation demand is estimated to 216 hm^3/year (Table 1). In the Upper and Middle courses, the irrigation demand is merely fulfilled through pumping, whereas in the Lower river course, both surface water and groundwater abstractions take place. More precisely, during the irrigation period, the discharge of Boeoticos Kephisos is regulated through a system of locks, which divert water to the main irrigation channels. This results to practically zero inflows to Lake Yliki during summer. If surface water resources are insufficient, the deficit is fulfilled via pumping from nearby aquifers and Lake Yliki.

It is obvious that the development of a simulation model for the Boeoticos Kephisos water resource system is a challenging task. This is justified by both the complexity of the related physical processes (mainly due to the dynamics of the karst and the underground losses) and the existence of combined uses. We have to point out that, although this watershed is one of the most studied in Greece – the first studies were carried out at the end of 19th century –, no attempt was made towards an integrated approach. Moreover, the estimations regarding the basin's water potential are characterized by considerable disagreements.

Model formulation and input data

When formulating a conceptual model, an essential option is to calibrate as many parameters as the available information can support. Results from previous research suggest that, in case of hydrological modeling, up to five or six parameters can be identified from a timeseries of observed series (i.e., streamflow), using a traditional curve-fitting procedure (e.g., Wagener *et al.*, 2001).

This principle of parsimony was applied by taking into account the available hydrologic data of the watershed. This consists of daily discharge measurements at the basin outlet (Karditsa tunnel), semi-monthly discharge measurements at the main karstic springs and non-systematic level observations at a relatively small number of wells, mostly located in the plain areas of the watershed. Except for the discharge record at the outlet, which is the longest one in Greece – measurements exist from the beginning of the 20th century –, the rest of data was systematically available for a much shorter period, i.e. 1984-1994. Nevertheless, this period can be assumed representative of the hydrologic regime of the basin, because it contains both high- and low-flow periods, including the severe drought mentioned before. Moreover, within this period the water supply boreholes at Vassilika-Parori were drilled and operated intensively, by a rate of 50 hm^3/year.

The simulation model structure was constructed based on the physical characteristics of the watershed and its underlying aquifer. Specifically, for the simulation of the surface hydrological processes, the watershed was divided in two hydrologic response units (HRUs). This discretization is in accordance with the catchment terrain and geological properties; the first HRU (shaded area of Figure 5) has an area of 649 km^2 that corresponds to the karstic, mountainous part of the basin,

whereas the second one (white area of Figure 5), has an area of 1339 km^2 that corresponds to the basin's alluvial plains. The total number of parameters is 9, namely the four parameters of each soil moisture reservoir (K_1, K_2, λ, μ) and the upper bound ε, assumed common for the two HRUs.

On the other hand, for the simulation of the groundwater processes, the aquifer was represented through a grid of $4 \times 4 = 16$ cells, illustrated in Figure 6, left. Cells (1, 1) and (2, 4) correspond to groundwater tanks whose inflows represent the basin leakages to the sea. Cells (1, 4), (3, 4) and (4, 4), illustrated with dotted lines, correspond to dummy tanks of zero area that are set for convenience (i.e., to run the numerical solving scheme that imposes a rectangle multi-cell grid). The main karstic springs of the basin, for which there exist systematic discharge measurements, were grouped and represented by tanks corresponding to respective cells. Specifically, cell (4, 1) corresponds to the springs of Lilea and its surrounding region, cell (4, 2) corresponds to Mavroneri springs, cell (1, 3) corresponds to Melas and Polygyra springs (assumed merged), and cell (4, 3) corresponds to Erkina springs. The tanks corresponding to cells that are marked gray are supplied by the percolation of HRU 1, namely the karstic, mountainous areas of the basin that contribute directly to the spring yield. Similarly, cells (2, 1), (2, 2) and (2, 3) are supplied by the percolation of HRU 2, namely the plain areas of the basin. The arrows in Figure 6 represent the prevailing groundwater flow directions, and at each one corresponds a conductivity term. The total number of the groundwater model parameters is 13, namely 12 conductivities and the specific yield, assumed common for the whole aquifer, for reasons of parsimony. All tank heights were set equal to the average aquifer thickness (230 m). The initial water levels of all tanks representing springs was set equal to the spring altitude, whereas for the tanks representing the sea this was set to zero. Finally, for the rest of groundwater tanks, the initial levels were chosen to be consistent with the historical observations and the steady-state solution.

In Figure 6 (right), a coarse representation of the hydrosystem is illustrated, consisting of the main branch of Boeoticos Kephisos river, its main tributaries, supplied by the four karstic springs, and five borehole groups. Specifically, borehole groups 1 to 4 are used for irrigation, as explained in Table 1, whereas group 5, set just upstream of Mavroneri springs, correspond to Vassilika-Parori boreholes that are used for the water supply of Athens. Groundwater abstractions from each borehole group are made from the corresponding tank, according to the priorities of Table 1.

The model was calibrated on six years (October 1984-September 1990) and validated on four years (October 1990-September 1994). For the former period, there exist semi-monthly discharge measurements at all spring sites, whilst for the latter there exist less systematic measurements. This raw data was used to construct monthly runoff records for the four springs; their average annual values are shown in Table 2. Other input series were the demand for irrigation, the areal precipitation and the potential evapotranspiration. The precipitation of HRU 1 was estimated via the point rainfall samples of seven rain gauges lying at altitude more than 350 m, whereas the precipitation of HRU 2 was estimated via the point rainfall samples of five rain gauges of lower altitude (the average altitude of the watershed is about 480 m, with maximum 2457 m). The corresponding mean annual values for the whole control period are 707 mm (458 hm^3) and 622 mm (832 hm^3). Finally, the potential evapotranspiration was estimated using the Penman method.

Model calibration

An automatic calibration procedure requires the specification of a goodness-of-fit measure between the simulated and the observed response series of the catchment (habitually, the runoff at its outlet), consisting the objective function of an optimization problem. It is now recognized that a parameter estimation based on a single performance measure is rather inadequate to simulate properly all important characteristics of the physical system that are reflected in the observations (Gupta *et al.*, 1998; Kuczera & Mroczkowski, 1998). On the other hand, the use of alternative goodness-of-fit criteria may lead to multiple optimal parameter sets, which provide equally satisfactory responses. Despite the progress made after three decades of research (e.g., Johnston & Pilgrim, 1976; Sorooshian & Gupta, 1983; Beven & Binley, 1992; Gupta *et al.*, 1998; Boyle *et al.*, 2000; Wagener *et al.*, 2001), the parameter estimation problem is still considered state-of-the-art. During the last years, research is focused on the application of vector optimization techniques, through the use of multiple performance criteria that measure either different aspects of the hydrograph or different watershed responses (e.g., Yapo *et al.*, 1998; Madsen, 2000). In that case, there exist significant trade-offs between the various objectives and no unique set of parameters is able to optimize them simultaneously. On the contrary, the solution to the calibration problem is a set of parameters that are, from a mathematical point-of-

view, equivalent (these consist the so-called Pareto set). Although the statistical characteristics of these solutions provide useful information about model uncertainty, only one of them must be finally selected if the model is to be employed in hydrological forecasting. In such cases, the choice of the best compromise set is either based on the experience of the hydrologist or on numerical criteria, such as a weighted utility function (Cohon, 1978, pp. 164-212).

The model efficiency was evaluated by considering multiple performance criteria that refer to the observed response series at the basin outlet (Karditsa tunnel) and the four springs. However, instead of employing multi-objective optimization, a scalar optimization approach was adopted, by aggregating the various criteria into a single objective function. This approach was preferred for practical reasons, since the model complexity as well as the existence of various performance components within the objective function (five fitting criteria and two penalty terms, as will explained bellow) would lead to a high-dimensional (i.e. 7D) Pareto front. Primary investigations indicated that there exists an enormous number of non-dominated parameter sets providing calibrations that are far away from the objectives of the study, i.e. relatively good predictions of the spring hydrographs but simultaneously bad prediction of the hydrograph at Karditsa tunnel or unrealistic parameter values. Moreover, a manual choice of the best compromise parameter set would be an extremely hard and time-consuming task. On the other hand, the adopted strategy, where all performance criteria were aggregated through the use of appropriate weighting coefficients, in addition to the empirical guidance of the optimization procedure that will be explained herein, ensured a relatively fast and reliable model calibration.

Initially, the objective function was formulated as the weighted sum of the determination coefficients of the five hydrographs. The determination coefficient, usually referred in hydrology literature as Nash-Sutcliffe measure (Nash & Sutcliffe, 1970), is a goodness-of-fit measure given by:

$$d = 1 - \frac{\sum_{i=1}^{n} (x_i - y_i)^2}{\sum_{i=1}^{n} (x_i - \overline{x})^2} \tag{8}$$

where x_i is the observed series, $\overline{x}$ is its average value, y_i is the simulated series and n is the time horizon. The determination coefficient d_j of each series j was multiplied by a weighting factor w_j. For the total runoff, the prediction of which stands as the main objective of the study, the weight was set equal to 6. Furthermore, for the Mavroneri springs flow, a reliable prediction of which is also important for the reasons explained earlier, the weight was set equal to 2. For the rest of springs, a unit weight was adopted. We recall that the total number of parameters is 22, namely 9 for the surface and 13 for the groundwater module. This number is in accordance to the principle of parsimony, given that the objective function consists of five goodness-of-fit measures. Therefore, there is sufficient information to explain the adopted parameterization.

Besides spring flow measurements, other useful raw data were the water table observations at a restricted number of wells. However, a direct incorporation of these measurements into the objective function was not feasible since these refer to the drill scale, while the simulated tank level series refer to the aquifer scale. But on the other hand, the observations indicate that during the whole calibration period the water table decline was negligible for the entire aquifer except for the vicinity of Mavroneri springs. This useful information, which is independent of the model scale, was taken into account by introducing a penalty term P_1, defined as the square difference between the initial and the final level of each tank regarding the whole calibration period, i.e. $(w_n - w_0)^2$. In that manner, it was ensured that the calibration would forbid the appearance of over-year trends in the simulated aquifer level series.

A major characteristic of the groundwater system dynamics was the occasional interruption of spring flows. During the control decade, this phenomenon was observed at all springs except those of Melas. A successful representation of a spring's intermittency was assumed a crucial factor of the model reliability. Hence, a second penalty term P_2 was introduced (by means of average square error), to prohibit the generation of runoff in case of spring interruption or the opposite. We note that the above penalty is additional to the error term already incorporated into the Nash-Suttclife measure; the latter is affected by measurement errors as well as errors due to the use of monthly runoff values based on sparse discharge measurements, whereas the penalty term is independent of such errors.

According to the above assumptions, the formulation of the objective function was:

$$f = \sum_{j=1}^{5} w_j d_j + \xi_1 P_1 + \xi_2 P_2 \quad (9)$$

where ξ_1 and ξ_2 are scalar coefficients, the value of which was let to change in order to generate alternative optimal parameter sets.

The calibration procedure followed a hybrid strategy based on a combination of automatic and manual methods; such strategies have proved very effective in case of complex hydrologic models (e.g., Boyle *et al.*, 2000; Eckhartd & Arnold, 2001). First, a "rough" calibration was employed, allowing a large variation of parameters. Several optimizations were carried out, by modifying the boundaries of the feasible parameter space and the weights ξ_1 and ξ_2 of the two penalty terms. In that manner, some characteristic regions of attraction corresponding to specific regions of the Pareto set were detected. Next, the optimization was let to seek for the global optimum of each region of attraction, already identified within the previous phase, by drastically restricting the feasible space. Throughout this phase, the calibration was separately performed for the surface and groundwater model parameters, in order to primarily ensure a very good adaptation of the hydrograph at the basin outlet, and secondly, an acceptable adaptation of the spring hydrographs. All optimizations were carried out via the evolutionary annealing-simplex algorithm, which proved very effective and efficient, taking into account the peculiarities of this problem. Moreover, the manual control of calibrations directed the algorithm to acceptable regions, which ensured a satisfactory model performance for the entire set of criteria, in spite of the various uncertainties concerning the physical processes, the relatively large number of parameters and their interactions, as well as the major approximations concerning the model inputs (e.g. the abstractions).

Analysis of results

As expected, a large number of parameter sets was found to provide almost equivalently good performance, according to numerical (curve fitting) criteria. Therefore, the selection of the best compromise set was based on empirical considerations. Specifically, we rejected all sets providing at least one of the following characteristics: (a) parameters with no physical sense; (b) bad performance regarding the reproduction of some of the observed runoff series, namely points lying on the boundaries of the Pareto set; (c) bad reproduction of output statistics. The last criterion refers to

response series except the calibrated ones, namely series for which there are no available measurements. By investigating the properties of those series (marginal statistics and existence of over-year trends), we both ensured a reliable reproduction of all physical processes of the basin and a realistic hydrologic balance of it.

After extended investigation, two parameter sets were finally detected, the values of which are illustrated in Table 3. These sets provide similar performance by means of both numerical and empirical criteria. Tables 4 and 5 illustrate the model efficiency values of the five hydrographs for the calibration and validation period. The determination coefficient for the runoff series at the basin outlet exceeds 92% for the calibration and 80% for the validation, thus ensuring a very satisfactory predictive capability of the model. Moreover, the bias referring to both the historical mean and standard deviation is negligible (about 1% and –4%, respectively, for both parameter sets). Although model efficiency regarding springs was not as good as the hydrograph at the outlet, this was still acceptable, given the complexity of the karstic system and the inaccuracies in the calibration data (hydrographs based on infrequent measurements). Even the performance of Melas-Polygyra springs is satisfactory, despite the fact that their historical runoff series present almost zero or even negative cross-correlation with precipitation. Figures 7 and 8 illustrate the observed and simulated hydrographs at the basin outlet and Mavroneri springs, respectively (for the entire time horizon). Although these hydrographs refer to the first parameter set, they are practically identical to those of the second one.

As shown in Table 3, some parameter values are almost identical for the two sets, thus indicating low uncertainty. But for others, the uncertainty remaining after the calibration is still significant; these are parameters mainly affecting the estimation of the evapotranspiration and outflows to the sea (e.g., conductivities upstream of tanks concentrating the losses to the sea). In reality, due to the existence of non-measurable outflows to the sea, the problem of allocating the hydrological losses of the basin is ill-posed, given that it has a degree of freedom. Table 6 shows the mean annual surface and groundwater hydrologic balance for the 10-year control period, which refers to the two parameter sets. In reality, these sets provide two extreme scenarios regarding the allocation of hydrological losses. Specifically, the first parameter set provides the highest (among the two) evapotranspiration (835 hm^3/year or 64.7% of the mean annual precipitation) and the lowest outflows

to the sea (61 hm^3/year), whereas the second set provides the lowest evapotranspiration (727 hm^3/year or 56.4% of the mean annual precipitation) and the highest outflows to the sea (182 hm^3/year). In the absence of further information, such as estimations based on direct measurements, any of the parameter sets is suitable for the purpose of the study.

SUMMARY AND CONCLUSIONS

The paper presents an integrated approach regarding conjunctive modeling of surface and groundwater hydrological processes, through a case study on a watershed with many peculiarities. In this study, the following issues are investigated: (a) building a model for simulating both physical processes and human interventions at the watershed scale; (b) developing an innovative optimization method for automatic model calibration; and (c) proposing a calibration strategy that used both manual and automatic procedures and was based on a combined optimization criterion, including various types of information on the system studied.

The hydrological simulator consists of three independent modules that were integrated within a conjunctive scheme. The first is a conceptual soil moisture accounting model, based on an enhanced version of the classical Thornthwaite approach. The model is able to represent the main hydrological processes, even when applied to a semi-arid catchment. The second module is a groundwater model based on a multi-cell approach that uses an explicit numerical scheme for the solution of flow equations. Its novelty is that, albeit using only two conceptual components (groundwater tanks and conveyance elements), it attains to represent all essential processes of a groundwater system, including spring runoff and water exchanges with neighboring aquifers (or the sea). The third module is a water management model, which is linked to the aforementioned ones in case of combined abstractions. Outputs of one model become inputs to the other; e.g., the percolation rates of the surface simulation model supplies the groundwater tanks, whereas the demand rates of the water management model are used to estimate surface and groundwater abstractions. The main advantage of the above scheme is that each of the three modules can be applied in different time and space scales. Moreover, although it uses relatively few parameters, it attains to represent particularly complex physical systems, even perturbed through human interventions.

For the automatic calibration of model parameters, an innovative method, the so-called evolutionary annealing-simplex algorithm, was used. This is a robust global optimization scheme, suitable for problems with rough response surfaces. This algorithm combines well-known methodologies, such as simulated annealing and the downhill simplex technique, within an evolutionary scheme. Its specific feature is the use of transition rules that are both deterministic and stochastic, where the degree of randomness is automatically adapted through a suitable annealing schedule; as the search proceeds, the influence of the stochastic component is gradually reduced until the global optimum is reached. The case study, also regarded as a benchmark test for the evolutionary annealing-simplex algorithm, provided encouraging conclusions about its performance; generally, both in terms of accuracy and speed, the algorithm proved practically equivalent to the widely used shuffled complex evolution method.

Our study indicated that, when calibrating hydrologic models, especially in case of complex simulation schemes with many parameters and multiple performance criteria, it is preferable to employ both automatic and manual methods. In that case, the hydrologist's experience is crucial regarding three issues: (a) the formulation of the objective function; (b) the guidance of the search procedure, through setting appropriate boundaries on parameters; (c) the selection of the best compromise solution. Regarding the first issue, it proved critical to take advantage of all available data reflecting the basin responses, thus using multiple performance criteria. Specifically, the model performance was tested on the basis of measured responses (i.e. hydrographs) and indicative but non-representative measures of model state variables (i.e. groundwater levels). Concerning the second issue, the shrinkage of the feasible space facilitates the search procedure and also leads to realistic parameter values. Finally, the third issue points out the importance of analyzing model outputs regarding not only the observed responses but also the non-observed series (i.e. evapotranspiration), and using empirical criteria in order to achieve realistic predictions. We also note that in the specific case study, the adopted scalar optimization strategy that involved our manual interventions proved much more convenient than typical multi-objective optimization approaches, since it avoided to explore a vast number of solutions that may be inconsistent with our objectives.

The application of the conjunctive model to the particularly complex Boeoticos Kephisos basin proved that, albeit using relatively few parameters and a coarse spatial analysis, the model managed to reliably represent not only the main responses of the catchment, i.e. the runoff at its outlet, but also other important components, concerning the dynamics of the underlying system. The model provided satisfactory predictions despite various uncertainties related to the complexity of the physical processes and the quality of input data. Moreover, due to its parsimonious formulation, the model was computationally quite effective. However, some weaknesses have been detected regarding the simultaneous calibration of parameters of different scales, e.g. reservoir capacities and conductivities. This problem is typical in conjunctive modeling and may be a possible issue for further research.

An appropriate implementation of the model presupposes, among others, the discrimination of the watershed and its underlying aquifer into spatial elements with homogenous characteristics, i.e. hydrologic response units and groundwater cells, respectively. Although in our case study this was done manually, the existence of a systematic procedure on formulating the model structure (based on criteria such as geology, geomorphology and land-use) not only would facilitate the user but also it would contribute to a more rational conceptualization. Other issues for further improvement of the model are: (a) the incorporation of routing procedures, in order to employ simulations at finer than monthly time step, (b) the use of a better (e.g. implicit) numerical scheme, in order to reduce the computational effort of groundwater simulation, and (c) the enhancement of the water management model, to represent more complex hydrosystems, consisting of reservoirs, river diversions, etc.

The calibration strategy may stand as a proposal for treating the equifinality problem in response to the need of a unique parameter set for engineering applications. Moreover, this strategy is consistent with the most recent approaches on multiobjective optimization, where decision-making is implemented in an interactive manner, by articulating preferences during the search; after each optimization step, a number of alternative solutions are obtained, on the basis of which the user specifies further preference information, thus guiding the search (Horn, 1997).

This paper mainly focused on the formulation and calibration of the hydrological model. The next step is to integrate this model within the DSS for the management of the Athens water supply

system, as explained in the introduction. Currently, our research team is working in this direction; the results will be reported in due course.

Acknowledgments The research of this paper was performed within the framework of the projects *Modernization of the supervision and management of the water supply system of Athens*, funded by the Water Supply and Sewerage Company of Athens (EYDAP), and *Integrated management of hydrosystems in conjunction with an advanced information system (ODYSSEUS)*, funded by the General Secretariat of Research and Technology, and both elaborated by the Department of Water Resources of the National Technical University of Athens. The authors wish to thank the directors of EYDAP and the members of the project committee for the support of the research. Thanks are also due to Elias Dandolos, director of the Institute of Geological and Mineral Exploitation, for providing useful information about the study area. Finally, the authors are grateful to two anonymous reviewers, for their positive comments that were very helpful for an improved presentation of the paper.

References

Bear, J. (1979) *Hydraulics of Groundwater*, McGraw-Hill, New York.

Beven, K. J. (1989) Changing ideas in hydrology – The case of physically-based models, *J. Hydrol.*, 105, 157-172.

Beven, K. J., & A. M. Binley (1992) The future of distributed models: model calibration and uncertainty prediction, *Hydrol. Processes*, 6, 279-298.

Boyle, D., H. V. Gupta, & S. Sorooshian (2000) Toward improved calibration of hydrologic models: Combining the strengths of manual and automatic methods, *Wat. Resour. Res.*, 36(12), 3663-3674.

Cohon, J. I. (1978) *Multiobjective Programming and Planning*, Academic Press, 1978.

Duan, Q., S. Sorooshian, & V. Gupta (1992) Effective and efficient global optimization for conceptual rainfall-runoff models, *Wat. Resour. Res.*, 28(4), 1015-1031.

Eckhartd, K., & J. G. Arnold (2001) Automatic calibration of a distributed catchment model, Technical note, *J. Hydrol.*, 251, 103-109.

Efstratiadis, A. (2001) *Investigation of global optimum seeking methods in water resources problems*, MSc thesis, 139 pages, Dept. of Water Resources, Nat. Tech. Univ. of Athens (full text in Greek; extended abstract in English, available at http://itia.ntua.gr/e/docinfo/446/).

Efstratiadis, A., & D. Koutsoyiannis (2002) An evolutionary annealing-simplex algorithm for global optimisation of water resource systems, *Proceedings of the 5th International Conference on Hydroinformatics*, Vol. 2, 1423-1428, Cardiff, UK, July 2002, IAHR, IWA, IAHS.

Franchini, M., G. Galeati, and S. Berra (1998) Global optimization techniques for the calibration of conceptual rainfall–runoff models, *Hydrol. Sci. J.*, 43(3), 443–458.

Gan, T., & G. Biftu (1996) Automatic calibration of conceptual rainfall-runoff models: Optimization theories, catchment conditions and model structure, *Wat. Resour. Res.*, 32(12), 3513-3524.

Gupta, H. V., S. Sorooshian, & P. O. Yapo (1998) Toward improved calibration of hydrologic models: Multiple and non-commensurable measures of information, *Wat. Resour. Res.*, 34(4), 751-763.

Horn, J. (1997) Multicriteria decision making, in T. Back, D. B. Fogel, and Z. Michalewicz (Eds.), *Handbook of Evolutionary Computation*, Bristol (UK), Institute of Physics Publishing.

Johnston, P. R., & D. Pilgrim (1976) Parameter optimization for watershed problems, *Wat. Resour. Res.*, 12(3), 477-486.

Koukis, G. C., & D. Koutsoyiannis (1997) *Greece, Geomorphological hazards in Europe*, edited by C.&C. Embleton, 215-241.

Koutsoyiannis, D., A. Efstratiadis, & G. Karavokiros (2002) A decision support tool for the management of multi-reservoir systems, *J. Amer. Wat. Res. Assoc.*, 38(4), 945-958.

Kuczera, G., & M. Mroczkowski (1998) Assessment of hydrologic parameter uncertainty and the worth of multiresponse data, *Wat. Resour. Res.*, 34(6), 1481-1489.

Kvasnicka, V., & J. Pospichal (1997) A hybrid of simplex method and simulated annealing, *Chemometrics and Intelligent Laboratory Systems*, 39, 161-173.

Madsen, H. (2000) Automatic calibration of a conceptual rainfall-runoff model using multiple objectives, *J. Hydrol.*, 235(4), 276-288.

Makhlouf, Z., and C. Michel (1994) A two-parameter monthly water balance model for French watersheds, *J. Hydrol.*, 162, 299-318.

Nalbantis, I., & E. Rozos (2000) A system for the simulation of the hydrological cycle in the Boeoticos Kephisos Basin, *Modernization of the supervision and management of the water resource system of Athens*, Report 10, 72 pages, Dept. of Water Resources, Nat. Tech. Univ. of Athens.

Nalbantis, I., E. Rozos, G. Tentes, A. Efstratiadis, & D. Koutsoyiannis (2002) Integrating groundwater models within a decision support system, *Proceedings of the 5th International Conference of European Water Resources Association: "Water Resources Management in the Era of Transition"*, edited by G. Tsakiris, Athens, 4-8 September 2002, 279-286, EWRA, IAHR.

Nash, J. E., & J. V. Sutcliffe (1970) River flow forecasting through conceptual models, I, A discussion of principles, *J. Hydrol.*, 10(3), 282-290.

Nelder, J., & R. Mead (1965) A simplex method for function minimization, *Comp. J.*, 7(4), 308-313.

Pan, L., & L. Wu (1998) A hybrid global optimization method for inverse estimation of hydraulic parameters: annealing-simplex method, *Wat. Resour. Res.*, 34(9), 2261-2269.

Press, W. H., S. A. Teukolsky, W. T. Vetterling, & B. P. Flannery (1992) *Numerical Recipes in C*, Second edition, Camb. Univ. Press, Cambridge, UK.

Sorooshian, S., & V. Gupta (1983) Automatic calibration of conceptual rainfall-runoff models: The question of parameter observability and uniqueness, *Wat. Resour. Res.*, 19(1), 260-268.

Thornthwaite, C. W. (1948) An approach toward a rational classification of climate. *Geogr. Rev.*, 38(l), 55-94.

Thornthwaite, C. W., and J. R. Mather (1955) The water balance, *Publ. Climatol. Lab. Climatol. Dresel Inst. Technol*., 8(8), 1-104.

Thyer, M., G. Kuczera, & B. C. Bates (1999) Probabilistic optimization for conceptual rainfall-runoff models: A comparison of the shuffled complex evolution and simulated annealing algorithms, *Wat. Resour. Res.*, 35(3), 767-773.

Wagener, T., D. P. Boyle, M. Lees, H. S. Wheater, H. V. Gupta, & S. Sorooshian (2001) A framework for development and application of hydrological models, *Hydrol. Earth Sys. Sci.*, 5(1), 13-26.

Xu, C.-Y., and V. P. Singh (1998) A review of monthly water balance models for water resources investigations, *Wat. Resour. Manag.*, 12, 31-50.

Yapo, P. O., H. V. Gupta, & S. Sorooshian (1998) Multi-objective global optimization for hydrologic models, *J. Hydrol.*, 204, 83-97.

Tables

Table 1 Allocation of irrigation demand, ordered by priority.

Irrigated region	Area (km^2)	Abstractions from	Demand (hm^3/year)
Upstream boundaries until Mavroneri springs	19	Aquifers (borehole group 1)	13
Mavroneri springs region	51	Mavroneri springs Aquifers (borehole group 2)	34
Between Mavroneri and Melas springs	29	Aquifers (borehole group 3)	19
Downstream of Melas springs	226	Lake Yliki (≈ 20 hm^3) Streamflow diversions Aquifers (borehole group 4)	150
TOTAL	325		216

Table 2 Mean annual runoff of Boeoticos Kephisos river and its springs (hm^3).

Runoff series	Calibration period (10/1984-9/1990)	Validation period (10/1990-9/1994)
Lilea springs	34.8	Not available
Mavroneri springs	48.4	27.2
Melas-Polygyra springs	123.7	Not available
Erkina springs	21.0	Not available
Net runoff at Karditsa tunnel	233.9	171.6

Table 3 List of calibrated model parameters.

Parameter	Symbol	Unit	Set 1	Set 2
Interflow threshold for HRU 1	$K_1(1)$	m	0.037	0.019
Interflow threshold for HRU 2	$K_1(2)$	m	0.331	0.331
Storage capacity of HRU 1	$K_2(1)$	m	0.167	0.132
Storage capacity of HRU 2	$K_2(2)$	m	0.442	0.589
Interflow retention rate of HRU 1	$\lambda(1)$	month $^{-1}$	0.068	0.078
Interflow retention rate of HRU 2	$\lambda(2)$	month $^{-1}$	0.043	0.042
Percolation retention rate of HRU 1	$\mu(1)$	month $^{-1}$	0.359	0.452
Percolation retention rate of HRU 2	$\mu(2)$	month $^{-1}$	0.056	0.089
Upper bound of potential evapotranspiration	ε	month $^{-1}$	0.232	0.213
Specific yield (common for the entire aquifer)	S_Y	month $^{-1}$	0.274	0.171
Conductivity from cell (1,2) to (1,1)	$C_x(1,1)$	m/s	0.000025	0.000023
Conductivity form cell (2,1) to (2,2)	$C_x(2,1)$	m/s	0.000275	0.000471
Conductivity form cell (1,2) to (1,3)	$C_x(1,2)$	m/s	0.020333	0.008856
Conductivity from cell (2,2) to (2,3)	$C_x(2,2)$	m/s	0.000067	0.002120
Conductivity form cell (2,3) to (2,4)	$C_x(2,3)$	m/s	0.000127	0.000414
Conductivity from cell (3,1) to (2,1)	$C_y(2,1)$	m/s	0.000033	0.000043
Conductivity from cell (3,1) to (4,1)	$C_y(3,1)$	m/s	0.010815	0.005089
Conductivity from cell (2,2) to (1,2)	$C_y(1,2)$	m/s	0.001712	0.001931
Conductivity from cell (3,2) to (3,3)	$C_y(2,2)$	m/s	0.000066	0.000096
Conductivity from cell (3,2) to (4,2)	$C_y(3,2)$	m/s	0.006275	0.003562
Conductivity from cell (3,3) to (2,3)	$C_y(2,3)$	m/s	0.000005	0.000007
Conductivity from cell (3,3) to (4,3)	$C_y(3,3)$	m/s	0.000862	0.000562

Table 4 Model efficiency, by means of determination coefficients for the calibration and validation periods (NSCAL and NSVAL, respectively) and relative error of average and standard deviation (AVERR and STDERR, respectively) for the calibration period – Parameter set 1.

Runoff series	NSCAL	NSVAL	AVERR	STDERR
Basin outlet	0.926	0.803	0.011	-0.041
Lilea springs	0.795	0.522	0.054	-0.069
Mavroneri springs	0.659	0.495	-0.069	-0.299
Melas-Polygyra springs	0.194	-	-0.029	-0.301
Erkina springs	0.358	0.254	0.001	-0.303

Note: The determination coefficients of the spring hydrographs are not corresponding to the entire validation period (48 months), but to a smaller one (34 months for Lilea and Mavroneri springs, 30 months for Erkina springs, and none for Melas and Polygyra springs).

Table 5 Model efficiency, by means of determination coefficients for the calibration and validation periods (NSCAL and NSVAL, respectively) and relative error of average and standard deviation (AVERR and STDERR, respectively) for the calibration period – Parameter set 2.

Runoff series	NSCAL	NSVAL	AVERR	STDERR
Basin outlet	0.922	0.801	-0.009	-0.036
Lilea springs	0.805	0.527	0.015	-0.131
Mavroneri springs	0.688	0.469	-0.059	-0.286
Melas-Polygyra springs	0.249	-	-0.021	-0.452
Erkina springs	0.354	0.258	-0.005	-0.227

Table 6 Mean annual water balance of Boeoticos Kephisos catchment (hm^3).

Hydrologic variable	Parameter set 1	Parameter set 2
Surface water balance		
Precipitation	1291 (100.0%)	1291 (100.0%)
Actual evapotranspiration	835 (64.7%)	727 (56.4%)
Percolation	342 (26.5%)	457 (35.5%)
Flood runoff	114 (8.8%)	109 (8.4%)
Groundwater balance		
Percolation	342 (100.0%)	457 (100.0%)
Spring runoff	192 (56.0%)	192 (42.0%)
Pumping	134 (39.1%)	133 (29.0%)
Underground flows to the sea	61 (17.8%)	182 (39.7%)
Groundwater storage difference	-44 (-12.9%)	-49 (-10.7%)
Water abstractions		
Surface water abstractions	83 (38.3%)	84 (38.7%)
Groundwater abstractions (pumping)	134 (61.7%)	133 (61.3%)
Total abstractions	217 (100.0%)	217 (100.0%)
Hydrological losses		
Evapotranspiration	835 (93.2%)	727 (80.0%)
Outflows to the sea	61 (6.8%)	182 (20.0%)
Total losses	896 (100.0%)	909 (100.0%)
Boeoticos Kephisos runoff		
Total runoff	306 (100.0%)	301 (100.0%)
Surface water abstractions	83 (27.1%)	84 (27.8%)
Net runoff (Karditsa tunnel)	223 (72.9%)	217 (72.2%)

Figure captions

Fig. 1 Original (left) and modified (right) Thornthwaite model.

Fig. 2 Groundwater model tanks.

Fig. 3 An example of establishing a scheme for combined simulation of surface and groundwater flows.

Fig. 4 Schematic representation of simplex configurations in a two-dimensional search space: (a) reflection, (b) expansion, (c) outside contraction, (d) inside contraction, (e) shrinkage. Solid lines correspond to the initial configuration, whereas dashed ones correspond to the final configuration.

Fig. 5 The Boeoticos Kephisos river basin, its main karstic springs and the water supply boreholes at Vassilika-Parori. The shaded area represents the mountainous regions of the basin and corresponds to HRU 1, whereas the white one represents the plain regions and corresponds to HRU 2.

Fig. 6 Illustration of the multi-cell groundwater simulation model (left) and the hydrosystem schematization (right). The aquifer bounds are represented by the thick frame. Gray cells correspond to mountainous karstic regions whereas white ones correspond to plain regions, and they are supplied by the percolation of HUR 1 and HRU 2, respectively. Dummy cells are illustrated with dotted lines. On the left figure, arrows represent feasible water paths between groundwater tanks; at each one corresponds a specific conductivity value. Circles represent springs, whereas triangles (on the right scheme) represent groundwater abstractions from the corresponding borehole groups (Table 1).

Fig. 7 Observed and simulated time series of the monthly runoff at the basin outlet (Karditsa tunnel), from October 1984 to September 1994 (parameter set 1).

Fig. 8 Observed and simulated time series of the mean monthly discharge of Mavroneri springs, from October 1984 to September 1994 (parameter set 1).

Figures

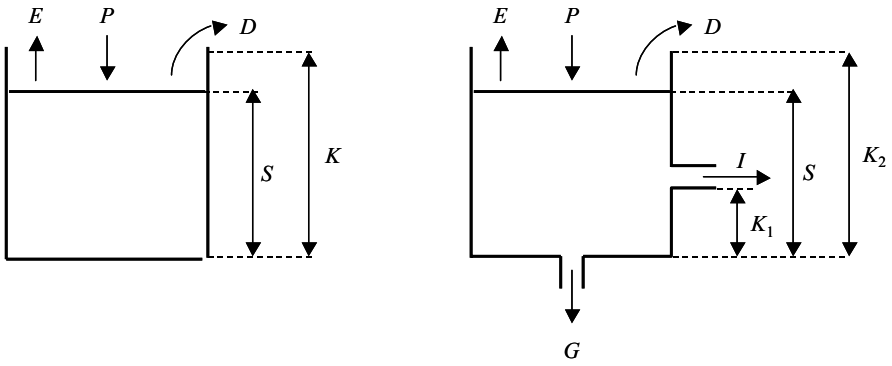

Fig. 1 Original (left) and modified (right) Thornthwaite model.

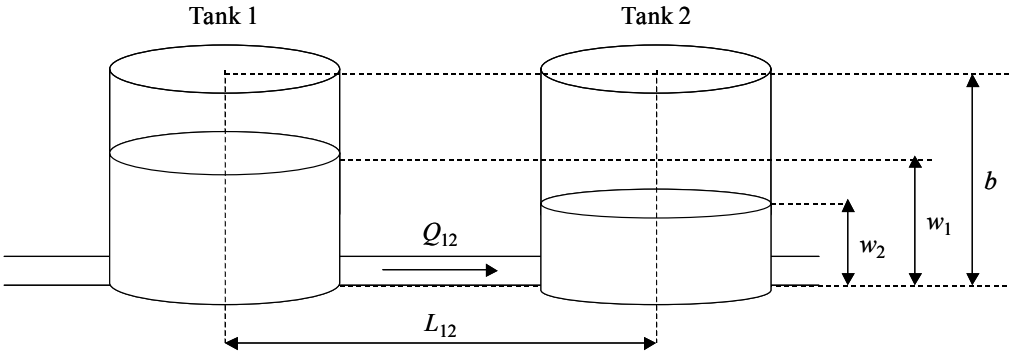

Fig. 2 Groundwater model tanks.

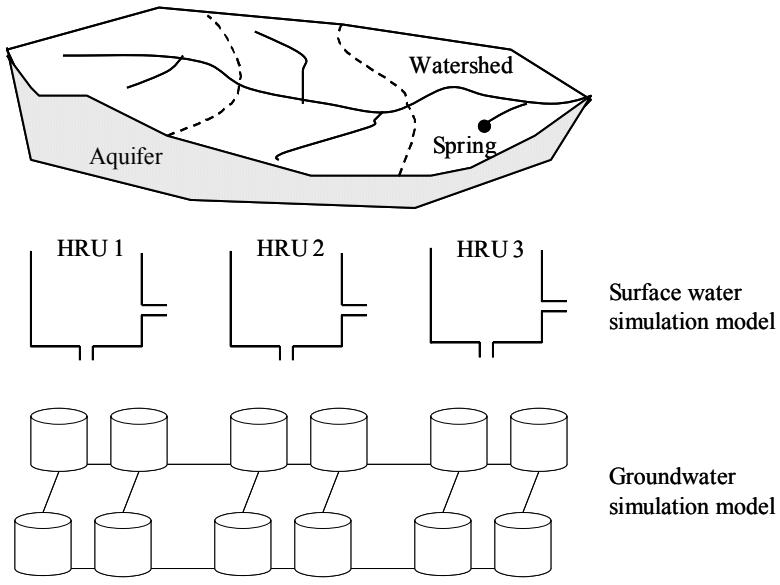

Fig. 3 An example of establishing a scheme for combined simulation of surface and groundwater flows.

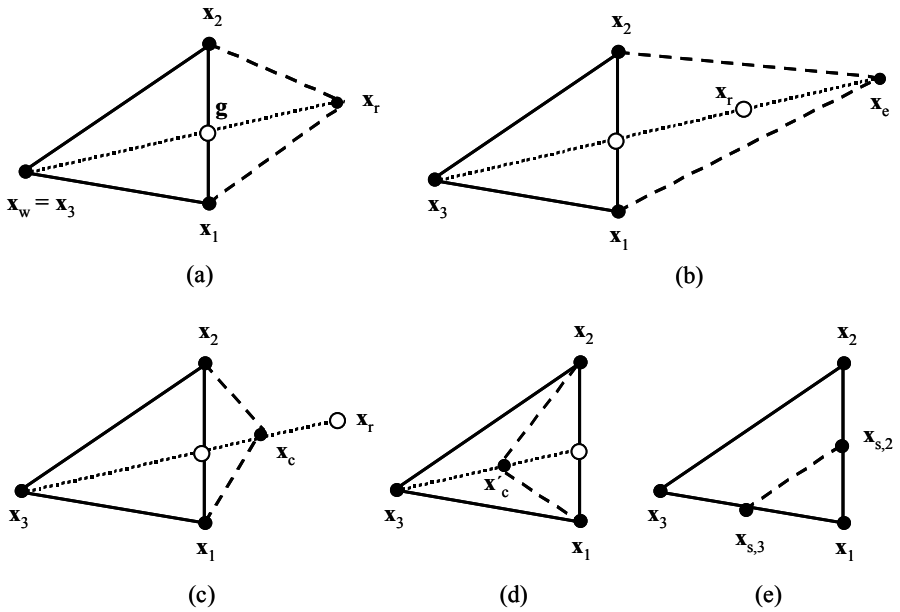

Fig. 4 Schematic representation of simplex configurations in a two-dimensional search space: (a) reflection, (b) expansion, (c) outside contraction, (d) inside contraction, (e) shrinkage. Solid lines correspond to the initial configuration, whereas dashed ones correspond to the final configuration.

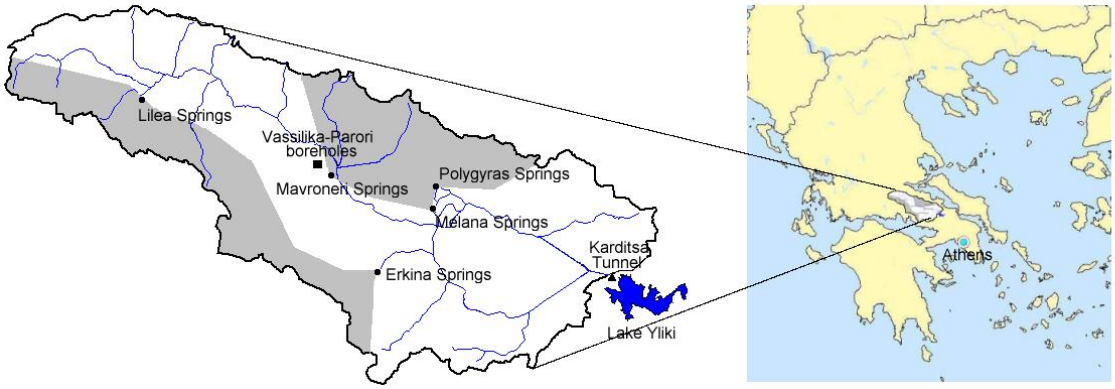

Fig. 5 The Boeoticos Kephisos river basin, its main karstic springs and the water supply boreholes at Vassilika-Parori. The shaded area represents the mountainous regions of the basin and corresponds to HRU 1, whereas the white one represents the plain regions and corresponds to HRU 2.

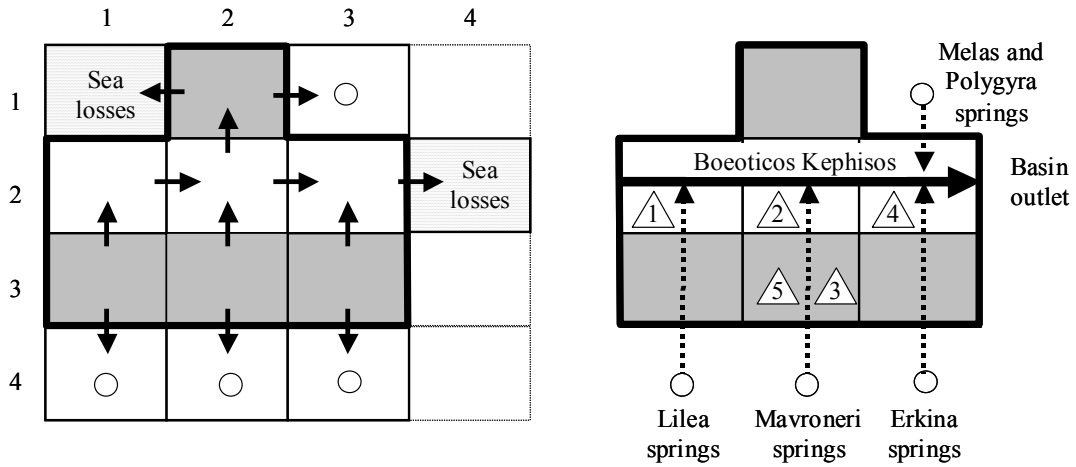

Fig. 6 Illustration of the multi-cell groundwater simulation model (left) and the hydrosystem schematization (right). The aquifer bounds are represented by the thick frame. Gray cells correspond to mountainous karstic regions whereas white ones correspond to plain regions, and they are supplied by the percolation of HUR 1 and HRU 2, respectively. Dummy cells are illustrated with dotted lines. On the left figure, arrows represent feasible water paths between groundwater tanks; at each one corresponds a specific conductivity value. Circles represent springs, whereas triangles (on the right scheme) represent groundwater abstractions from the corresponding borehole groups (Table 1).

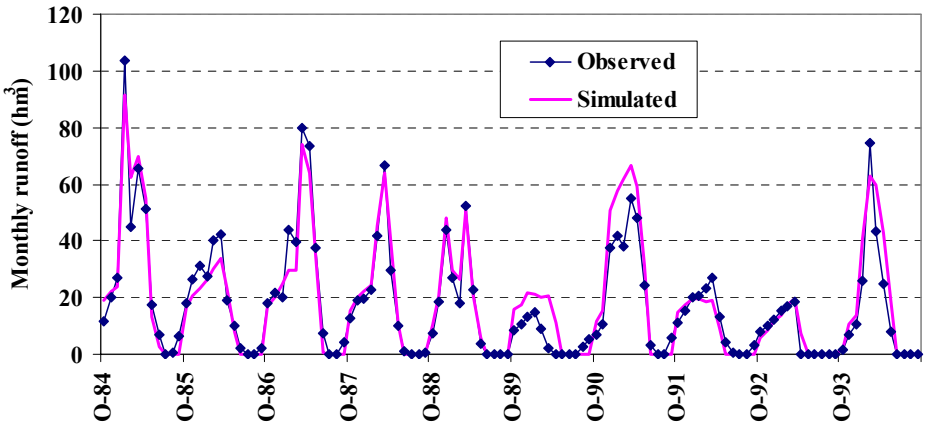

Fig. 7 Observed and simulated time series of the monthly runoff at the basin outlet (Karditsa tunnel), from October 1984 to September 1994 (parameter set 1).

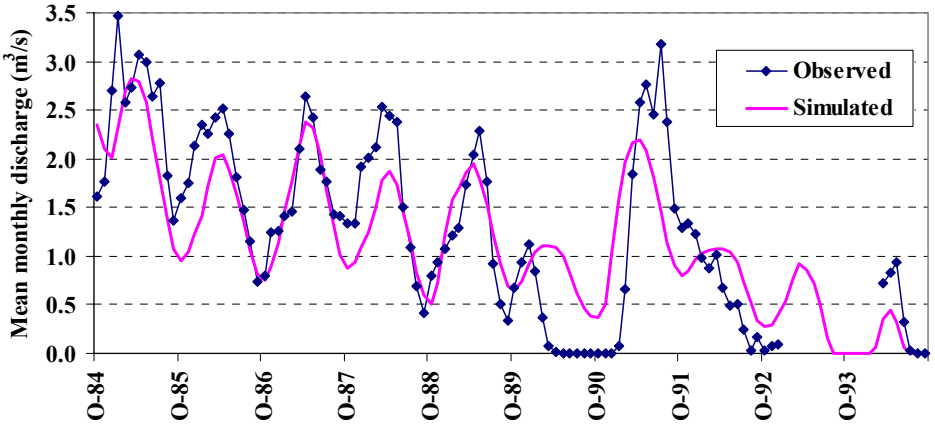

Fig. 8 Observed and simulated time series of the mean monthly discharge of Mavroneri springs, from October 1984 to September 1994 (parameter set 1).